Experimental study on the heat transfer characteristics of a low melting point salt in a parabolic trough solar collector system

Wu, Yu-ting; Liu, Shan-wei; Xiong, Ya-xuan; Ma, Chong-fang; Ding, Yulong

DOI:
10.1016/j.applthermaleng.2015.06.054

Accepted Manuscript

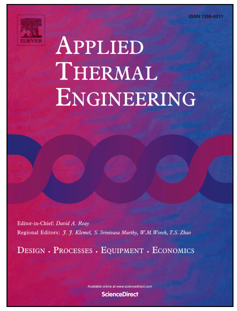

Experimental Study on the Heat Transfer Characteristics of a Low Melting Point Salt in a Parabolic Trough Solar Collector System

Yu-Ting Wu, Shan-Wei Liu, Ya-Xuan Xiong, Chong-Fang Ma, Yu-Long Ding

PII: S1359-4311(15)00612-2
DOI: 10.1016/j.applthermaleng.2015.06.054
Reference: ATE 6746

To appear in: *Applied Thermal Engineering*

Received Date: 10 January 2015
Revised Date: 6 June 2015
Accepted Date: 13 June 2015

Please cite this article as: Y.-T. Wu, S.-W. Liu, Y.-X. Xiong, C.-F. Ma, Y.-L. Ding, Experimental Study on the Heat Transfer Characteristics of a Low Melting Point Salt in a Parabolic Trough Solar Collector System, Applied Thermal Engineering (2015), doi: 10.1016/j.applthermaleng.2015.06.054.

Experimental Study on the Heat Transfer Characteristics of a Low Melting Point Salt in a Parabolic Trough Solar Collector System

Yu-Ting Wu[1], Shan-Wei Liu[1], Ya-Xuan Xiong[2], Chong-Fang Ma[1], Yu-Long Ding[3]

[1] Key Laboratory of Enhanced Heat Transfer and Energy Conservation, Ministry of Education and Key Laboratory of Heat Transfer and Energy Conversion, Beijing municipality, Beijing University of Technology, Beijing 100124, China.

[2] Key lab of HVAC, Beijing University of Civil Engineering and Architecture，100044, China.

[3]School of Chemical Engineering/Birmingham Centre of Cryogenic Energy Storage, University of Birmingham, B152TT United Kingdom.

Abstract：

An experimental system of parabolic trough solar collector and heat transfer was set up with a new molten salt employed as the heat transfer medium (with a melting point of 86℃ and a working temperature upper limit of 550℃). The circulation of molten salts in the system took place over 1,000 hrs. Experiments were conducted to obtain the heat loss of the Heat Collector Element (HCE), the total heat transfer coefficient of the water-to-salt heat exchanger, and the convective heat transfer coefficients for the low melting point molten salt in a circular tube. The results show that the thermal loss of the tested HCE is higher than that of the PTR70, and the thermal loss at the joints of the collector tube represents about 5% of the total loss in the entire tube. The total heat transfer coefficient of the water-to-salt heat exchanger was between 600 and 1200 W/(m^2·k) in the ranges of $10{,}000<Re<21{,}000$ and $9.5<Pr<12.2$. The experimental data show good agreement with existing well-known correlations presented by the Sieder-Tate equation and the Gnielinski equation. This experimental study on heat loss from molten salt flow in a receiver tube will hopefully serve as a helpful reference for applications in parabolic trough systems.

[1]Corresponding author. Tel.: +86-10-67391985-8323; Fax: +86-10-67392774

E-mail address: wuyuting1970@126.com (Yu-Ting Wu)

Keywords: low melting point molten salt; trough solar collector system; heat loss; heat transfer coefficient

1. Introduction

Nowadays, concentrated solar power (CSP) presents tremendous potential for the large-scale deployment of clean renewable energy [1], and it has been proven to be the most mature solar thermal technology available. As a result, most construction projects for commercial solar thermal power plants are currently based on this type of collector [2-4]. Many different kinds of working fluids are used in CSP systems [5-7], and selecting the appropriate heat transfer fluid and storage medium is a key technological issue for the future success of CSP technology. Molten salt represents an extremely promising medium for heat transfer and storage in CSP plants; its advantages include a wide working temperature range, low vapor pressure, large heat capacity, low viscosity, good chemical stability, and low cost [8-11]. Molten salt CSP storage was shown to be commercially viable in 2008, when the 50MWe Andasol-1 plant with 7.5 hours of molten salt storage began its operation [12]. However, the only CSP system that uses molten salt as the medium of heat transfer is the Archimede parabolic trough plant in Italy. In the Archimede system, the working fluid of the heat transfer and heat storage is solar salt that is a mixture of $NaNO_3$ and KNO_3 [13] with a high melting point(220℃). In such systems, the cost of operation will rise dramatically if there is an unexpected drop in temperature in the operating process in which the salt is used as the heat transfer fluid. Therefore, additional hard-ware must be installed, such as heat tracing, insulation, or emergency water-dilution systems. The high melting point is a major disadvantage of conventional molten salts and limits their application in trough CSP systems [3].

Based on different mixing ratios of KNO_3–$NaNO_3$–$LiNO_3$–$Ca(NO_3)_2 \cdot 4H_2O$, a new kind of nitrate salt was developed by our research group. Experimental results have shown that the melting point of this molten salt can be as low as 86℃ with a decomposition temperature above 600℃ [14]. Previous experiments have been carried out to obtain the convective heat transfer coefficients of the turbulent flow and transition flows of Hitec salts, $LiNO_3$, and fluoride salts in a circular tube [15-20]. However, heat transfer performance using a low melting point salt has not been reported in the literature.

A parabolic trough solar collector and heat transfer system was constructed at the end of 2011 with a low melting point molten salt [14]. Since then, numerous engineering issues have been addressed, such as the plugging of solidified molten salt, charging and discharging methods, equipment selection, and thermal and flow parameter measurements. A series of experiments on low melting point molten salt were conducted in the trough solar collector and heat transfer system, and the results of the experiments are reported in this paper. The heat loss of the HCE and the convective heat transfer coefficients of turbulent flows were obtained in a circular tube, and the total heat transfer coefficient of the water-to-salt heat exchanger was obtained as well.

2. Description of experimental system and working fluids

2.1 Experimental apparatus

A schematic diagram of the experimental system is shown in Fig. 1. The system contains molten salt circulation and water circulation. The main parts of the two cycles include a molten salt tank, a high-temperature molten salt pump, a molten salt heater, a concentrating collector, a water-to-salt heat exchanger, a water cooler, a water heater, a mass flow meter, and a water pump. The characteristics of the collector are presented in Table 1.

In order to avoid molten salt solidification in the tube, an automatic electric tracing band is utilized in the pipe system, the latter of which requires a certain lean of about 5‰. Due to the inherent properties of molten salts and the high temperature, most devices cannot effectively measure the molten salt flow. In order to measure the molten salt flow rates, many different types of flow meters were tested, such as target flow meters, mass flow meters, float flow meters, etc. Through comparative analysis, an ultrasonic flowmeter made by FLEXIM (Germany) was chosen to measure the flow rates of the molten salt, and a mass flow meter was installed in the water cycle. Meanwhile, the temperature of the molten salt was measured by a type K thermocouple with special limits of error(±1.1℃ or ±0.4% of the tested temperature, whichever is greater), and the temperature in the water cycle was measured with a PT100 resistance thermometer with an accuracy of 0.2℃. To obtain different flow rates of the molten salt, a frequency converter was installed to control the molten salt pump. Before the molten salt was pumped from the storage tank to the pipeline, the entire molten salt flow loop had to warm up. When the molten salt in the storage tank was heated to a prescribed temperature by an electric heater, the molten salt pump started to circulate the molten salt in the salt cycle.

2.2 Working fluids

A new kind of low melting point molten salt prepared by our lab [14] with a melting point of 86℃ and a working temperature upper limit of 550℃ was chosen as the working fluid in this experimental investigation. Its main thermophysical properties are listed in Table 2.

3. Results and discussion

3.1 Thermal loss of the HCE

In this parabolic trough solar system, the tested HCE features six evacuated collector tubes (each with a length of 2 m) welded together. Insulation with a length of 1.15m and a thickness of 40mm was adopted for proper heat preservation at the joints, including the bellows and the welding. The thermal loss of molten salt through the HCE can be calculated by the following equation:

$$q_{loss} = \dot{m} c_p (t_i - t_0) \quad (1)$$

where the thermal characteristic of the terminal through convection can be calculated as

$$q_c = hA(t_w - t_\infty) \quad (2)$$

and

$$h = Nu \frac{\lambda}{d} \quad (3)$$

When wind speed $V \le 0.1$m/s, Nu can be expressed as follows [21]:

$$Nu = \left\{ 0.6 + \frac{0.387 Ra^{1/6}}{\left[1 + (0.559 / \Pr)^{9/16}\right]^{8/27}} \right\}^2 \quad (4)$$

Once $V > 0.1$m/s, Nu is given as follows [21]:

$$Nu = C \operatorname{Re}^m \Pr^n \quad (5)$$

where $Pr \le 10$，n=0.37；$Pr > 0.36$，n=0.36. The values of C and m are listed in Table 3.

The thermal loss of the joints through radiation can be obtained as

$$Q_{rad} = A\sigma\varepsilon({t_w}^4 - {t_\infty}^4) \quad (6)$$

In order to eliminate the influence of sunlight, the experiments were carried out at night, and the maximum wind speed was less than 3 m/s. Fig. 2 shows the measured thermal heat loss through the HCE at different average fluid temperatures above the ambient air temperature. The results show that the thermal loss at the joints represents about 5% of the total thermal loss in the entire collector tube. However, it would reach 18% or so without any thermal insulation [22].

A comparison was also made between the present results and the data for a PTR70 receiver obtained in the same way but using oil as working fluid [23]. As shown in Fig. 3, the heat loss of the tested HCE is higher than that of the PTR70. One reason may be that the tested HCE had been operating at a high temperature (300℃~500℃) for two years, which may have damaged its coating to some degree.

3.2 Turbulent convective heat transfer with molten salt in a circular pipe

A type of double-pipe heat-exchanger was used in the experimental system, in which the high-temperature molten salt flowing inside the inner tube was cooled by low-temperature water flowing in the outer tube, as shown in Fig. 4. The diameter and thickness of the outer tube are 57mm and 3.5mm, respectively, while those of the inner tube are 32mm and 2mm, respectively; both tubes are 1,200mm long. The outer tube's surface was wrapped with insulation materials to minimize heat loss. By measuring the temperature at four points (i.e., water inlet, water outlet, molten salt inlet, and molten salt outlet) and calculating the heat loss of the tube, we were able to obtain the overall heat transfer coefficient from molten salt to water in the tested section.

The data processing method adopted in this experiment can be found in our previous work [15] on turbulent convective heat transfer coefficients of lithium nitrate in a circular tube. Using the same least-square methods, the overall heat transfer coefficients and the correlations were calculated for the convective heat transfer coefficients of low melting molten salts. Through analysis and derivation, we obtained the Nusselt number as follows:

$$Nu=0.0239Re^{0.804}Pr^{0.33} \quad (7)$$

Fig.5 shows that the total heat transfer coefficients increase within the a range of 600 to 1200 W/(m^2·k^1) as the molten salt temperature increases within a range of 14,000<Re<32,000. Fig. 6 illustrates the good agreement between the curve predicted by Eq. (7) and the experimental data, with a deviation of only ±7%; Eq. (7) is based on experimental data with Prandtl numbers ranging from 9.5 to 12.2. In order to verify the applicability of well-known convective heat transfer correlations in molten salts, five kinds of molten salts were identified from the literature [15-20] in ranges of 1.6<Pr<15.3 and

10,000<Nu<46,130. Figs. 7-9 show the comparisons between the present experimental results and the existing data for various equations.

From these figures, it can be seen that there is a relatively high deviation between experimental data from Kirst et al. [17] and the Dittus-Boelter equation, the Sieder-Tate equation [24], and the Gnielinski equation [25]. However, significant portions of the experimental data are quite consistent with the existing correlations. The maximum deviation between the present experimental results and the curves predicted by the Dittus-Boelter equation, Sieder-Tate equation [24], and Gnielinski equation [25] reach +23%, -10%, and -20% respectively. It is worth noting that the Sieder-Tate equation and the Gnielinski equation include property ratio correction terms and consider the effect of variable fluid properties, while the effect of thermo-physical property variation is not included in the Dittus-Boelter equation. In comparison, the present experimental results involve significant variation in the properties of molten salt. For example, when the temperature of the side wall of the molten salt is 175℃, its bulk temperature is 286℃, and the corresponding dynamic viscosity values are 4.83mPa·s and 3.34mPa·s respectively. This will yield distorted velocity and temperature fields, resulting in considerable changes in heat transfer performance compared to the case of constant properties. The good agreement between the present data and well-known turbulent convection correlations, including the Sieder-Tate equation and the Gnielinski equation, demonstrates the superior reliability of low melting point molten salts.

To highlight the influence of the Prandtl number, the present results and previous convective heat transfer data for various working fluids from the literature [15-20, 26] are compared in Fig. 10. Two curves predicted by the Dittus-Boelter equation, which represent fluid heating ($Pr^{0.4}$) and fluid cooling ($Pr^{0.3}$), are also presented in Fig. 10. It can be seen that most of the experimental data are congruent with the two curves, except for the data from Kirst et al. [17] and that of NaOH [26]. Clearly, the present experimental results are largely consistent with the experimental data collected from the literature [15-20, 26]. These comparisons demonstrate that the Prandtl number dependence provided by existing correlations is also applicable to molten salt convection.

Uncertainty analysis is necessary in order to validate the accuracy of the present experimental results. The uncertainties of the calculated results were evaluated using standard error analysis. In calculating the error in any measurement, both systematic and random errors must be accounted for. Systematic errors are related to instruments used in the measurements, and random errors concern data plots after the same measurements are repeated. In this experiment, the variables involved are temperature, flow rate, and wind speed. The random errors in this experiment are related to the scattering of data during the period of stable temperatures and flow rates. The random error for the calculated values of heat loss, specific heat, heat flux, heat transfer, and Nusselt number are calculated using the formula defined below:

$$\delta y = \sqrt{\left(\frac{\partial f}{\partial x_1}\delta x_1\right)^2 + \left(\frac{\partial f}{\partial x_2}\delta x_2\right)^2 + \cdots + \left(\frac{\partial f}{\partial x_n}\delta x_n\right)^2} \tag{8}$$

Specifically, the desired result is a well-behaved function $f(x_1, x_2, \cdots, x_n)$ of the direct physical variables (x_1, x_2, ..., x_n) that have uncertainties (δx_1, δx_2, …, δx_n). Then the equation can be written as

$$y = f(x_1, x_2, \cdots, x_n) \tag{9}$$

The errors of the calculated heat loss are presented in Table 4. It can be seen that the maximum and minimum error are ±3.18% and ±2.65%, respectively (in the first two experiments mentioned in this paper, the same temperature sensor and flow sensor were used). The errors of the measured and calculated parameters of the turbulent convective heat transfer are presented in Table 5. The errors of the calculated parameters are estimated to be ±9.6% for the total heat transfer coefficient, ±7.0% for the Nusselt number of molten salt, and ±9.3% for the heat flux between the water and molten salt.

4. Conclusions

(1) An experimental system consisting of a parabolic trough solar collector and heat transfer was set up with a new molten salt employed as the heat transfer medium (with a melting point of 86℃ and a working temperature upper limit of 550℃); The circulation of molten salts in the system took place over 1,000 hrs. The results indicated that operation, starting, and stopping the system using low melting point salts resulted in a lower risk of freezing and plugging compared with utilizing high melting point salts(e.g., solar salts).

(2) Experiments were conducted to obtain the thermal loss of the HCE as the temperature of the molten salt changed. The results were compared with the data for a PTR70 obtained in the same way but using oil as the working fluid. The results showed that the thermal loss of the tested tube was higher than that of the PTR70. Moreover, the thermal loss at the joints was about 5% of the total loss in the entire test collector tube, but if there was no thermal insulation, this proportion would reach about 18%.

(3) The total heat transfer coefficient of the water-to-salt heat exchanger was obtained for different temperatures and flow rates. The results showed that the total heat transfer coefficient of the water-to-salt heat exchanger ranged between 600 and 1200 W/(m^2·k) for $10,000<Re<21,000$ and $9.5<Pr<12.2$.

(4) The convective heat transfer coefficients and correlations for low melting point salts were calculated for 10,000<Re<21,000 and 9.5<Pr<12.2. Comparisons were made between the present experimental results and well-known empirical correlations. The present experimental data of convective heat transfer coefficients with low melting point molten salts demonstrated good agreement with the Sieder-Tate equation and the Gnielinski equation.

(5) The application of low melting point molten salts to CSP systems can help minimize operation

costs and required investment levels, and many practical engineering problems can be addressed easily. The experimental results will hopefully provide a helpful reference for the development of high-temperature molten salt CSP systems.

Acknowledgements

The authors are grateful for the financial support provided by the National Natural Science Foundation of China (Grant No. 51206004 and No. 51361135702), the National Basic Research Program of China (Grant No. 2015CB251303 and No. 2011CB707202), and the International S&T Cooperation Program of China (Grant No. 2014DF60600).

References

[1] X. L. Wei, Q. Peng, J. Ding, X. X. Yang, J. P. Yang, B. Long, Theoretical study on thermal stability of molten salt for solar thermal power, Appl. Therm. Eng. 54 (2013) 140-144.

[2] Z. Yang, V. S. Garimella, Thermal analysis of solar thermal energy storage in a molten-salt thermocline, Sol. Energy 84 (2010) 974-985.

[3] M. J. Montes, A. Abánades, J. M. Martínez-Val, M. Valdés, Solar multiple optimization for a solar-only thermal power plant, using oil as heat transfer fluid in the parabolic trough collectors, Sol. Energy 83 (2009) 2165-2176.

[4] L. Martín, M. Martín, Optimal year-round operation of a concentrated solar energy plant in the south of Europe, Appl. Therm. Eng. 59 (2013) 627-633.

[5] J. Pacio, C. Singer, T. Wetzel, R. Uhlig, Thermodynamic evaluation of liquid metals as heat transfer fluids in concentrated solar power plants, Appl. Therm. Eng. 60 (2013) 295-302.

[6] A. Rovira, M. J. Montes, F. Varela, M. Gil, Comparison of heat transfer fluid and direct steam generation technologies for integrated solar combined cycles, Appl. Therm. Eng. 52 (2013)

264-274.

[7] M. Mussard, O. J. Nydal, Comparison of oil and aluminum-based heat storage charged with a small-scale solar parabolic trough, Appl. Therm. Eng. 58 (2013) 146-154.

[8] D. Kearney, B. Kelly, U. Herrmann, Engineering aspects of a molten salt heat transfer fluid in a trough solar field, Energy 29 (2004) 861-864.

[9] M. S. Sohal, P. Sabharwall, P. Calderoni, Conceptual design of forced convection molten salt heat transfer testing loop, Report No. INL/EXT-10-19908, 2010, pp. 6-10.

[10] R. I. Olivares, The thermal stability of molten nitrite/nitrates salt for solar thermal energy storage in different atmospheres, Sol. Energy 86 (2012) 2576-2583.

[11] Y. J. Wang, Q. B. Liu, L. J. Lei, H. G. Jin, A three-dimensional simulation of a parabolic trough solar collector system using molten salt as heat transfer fluid, Appl. Therm. Eng. 70 (2014) 462-476.

[12] H. Michels, R. Pitz-Paal, Cascaded latent heat storage for parabolic trough solar power plants, Sol. Energy 81 (2007) 829-837.

[13] G. Glatzmaier, Summary report for concentrating solar power thermal storage workshop. Technical Report NREL/TP-5500-52134, August 2011.

[14] N. Ren, Y. T. Wu, C. F. Ma, L. X. Sang, Preparation and thermal properties of quaternary mixed nitrate with low melting point, Sol. Energy. Mat. Sol. Cells 127 (2014) 6-13.

[15] B. Liu, Y. T. Wu, C. F. Ma, M. Ye, H. Guo, Turbulent convective heat transfer with molten salt in a circular pipe, Int. Commun. Heat Mass 36 (2009) 912-916.

[16] H.W. Hoffman, J. Lones, Fused salt heat transfer, part II: forced convection heat transfer in circular tubes containing NaF-KF-LiF eutectic, Report No. ORNL-1777, 1955, pp. 5-25.

[17] H. W. Hoffman, S. I. Cohen, Fused salt heat transfer, part III: forced convection heat transfer in circular tubes containing the salt mixture NaNO2-KNO3-NaNO3, Report No. ORNL-2433,1960, pp. 9-13.

[18] M. D. Silverman, W. R. Huntley, H. E. Robertson, Heat Transfer Measurements in a forced convection loop with two molten-fluoride salts: LiF-BeF2-ThF4-UF4 and eutectic NaBF4-NaF, Report No. ORNL/TM-5335, 1976, pp. 16-21.

[19] Y. T. Wu, B. Liu, C. F. Ma, H. Guo, Convective heat transfer in the laminar-turbulent transition region with molten salt in a circular tube, Exp. Therm. Fluid. Sci. 33 (2009) 1128-1132.

[20] Y. T. Wu, C. Chen, B. Liu, C. F. Ma, Investigation on forced convective heat transfer of molten salts in circular tubes, Int. Commun. Heat Mass 39(10) (2012) 1550-1555.

[21] F. P. Incropera, D. P. DeWitt, Fundamentals of heat and mass transfer, third edition, New York: John Wiley and Sons, 1990.

[22] T. Wendelin, SolTrace: A new optical modeling tool for concentrating solar optics, Proceedings of the ISEC, Hawaii, 2003.

[23] Sandia Corporation, Final test results for the Schott HCE on a LS-2 Collector, Sandia National Laboratory, 2005.

[24] J. P. Holman, Heat Transfer, ninth edition, New York, 2002, pp. 261-270.

[25] V. Gnielinski, New equations for heat and mass transfer in turbulent pipe and channel flow, Int. Chem. Eng. 16(2) (1976) 359-367.

[26] D. F. Dipprey, An experimental investigation of heat and momentum transfer in smooth and rough tubes at various Prandtl numbers, PhD thesis, California Institute of Technology,

Pasadena, California, 1961.

Nomenclature

□, m mass flow rate, (kg/s)

A heat transfer area, (m^2)

Cp specific heat, (kg/(kg·K))

t temperature, (K)

h heat transfer coefficient, (W/(m^2·K))

Nu Nusselt number (hl/k)

Pr Prandtl number (ν/a)

Ra Rayleigh number

d diameter, (m)

L length, (m)

Greek symbols

λ thermal conductivity, (W/(m·K))

σ radiation constant, (W/(m^2·K^4))

ε emissivity

Subscripts

i inlet parameters, inner side parameters

o outlet parameters, outer parameters

s parameters of molten salt

w parameters of water, parameters of tube wall

∞ parameters of surroundings

Figure captions:

Fig. 1. Parabolic trough solar collector and heat transfer system with molten salt

Fig. 2. Thermal loss of the HCE and terminal

Fig. 3. Comparison between experimental results and the PTR70

Fig. 4. Schematic of the double-pipe heat exchanger

Fig. 5. Total heat transfer coefficient of the exchanger as the salt *Re* changes

Fig. 6. Fitting curve of the molten salt *Nu* and relative errors

Fig. 7. Comparison of present experimental results, existing data, and the Dittus-Boelter equation

Fig. 8. Comparison of present experimental results, existing data, and the Sieder-Tate equation

Fig. 9. Comparison of present experimental results, existing data, and the Gnielinski equation

Fig. 10. Prandtl number dependence of the Nusselt number of turbulent flow in a circular tube

List of Figures

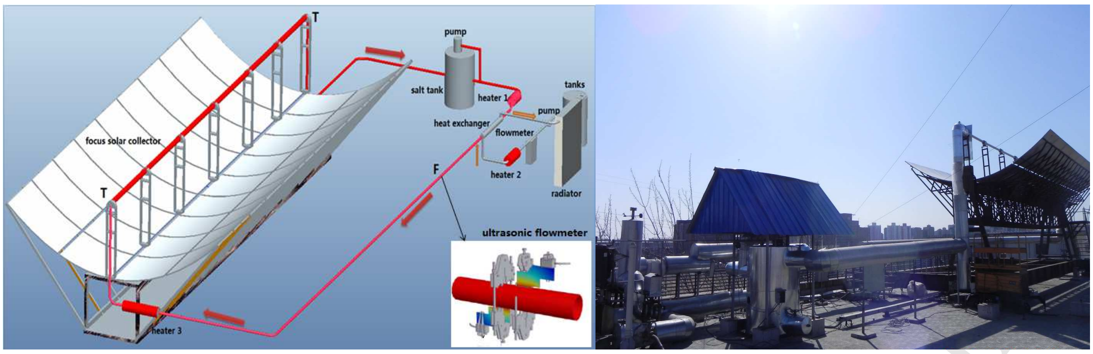

Fig. 1. Parabolic trough solar collector and heat transfer system with molten salt

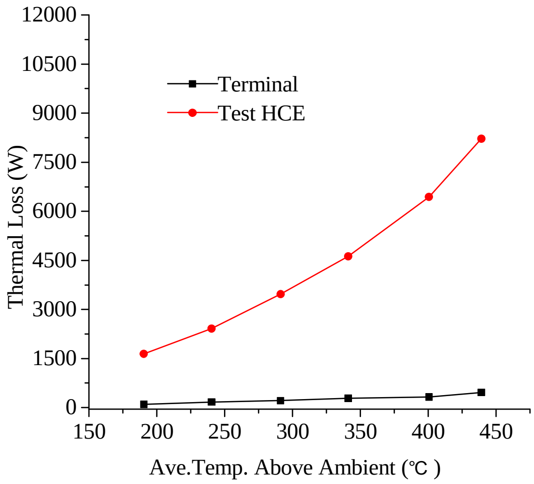

Fig. 2. Thermal loss of the HCE and terminal

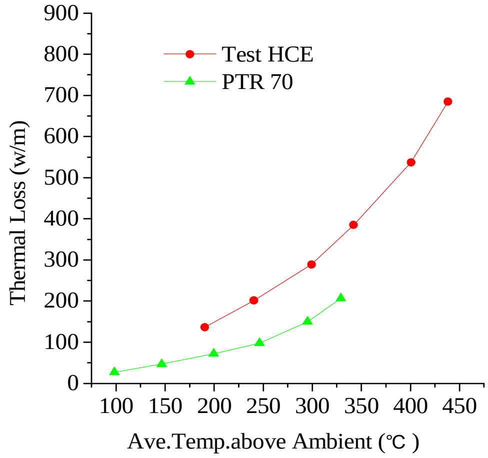

Fig. 3. Comparison between experimental results and the PTR70

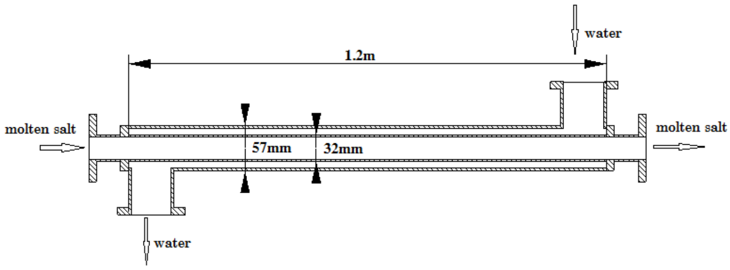

Fig. 4. Schematic of the double-pipe heat exchanger

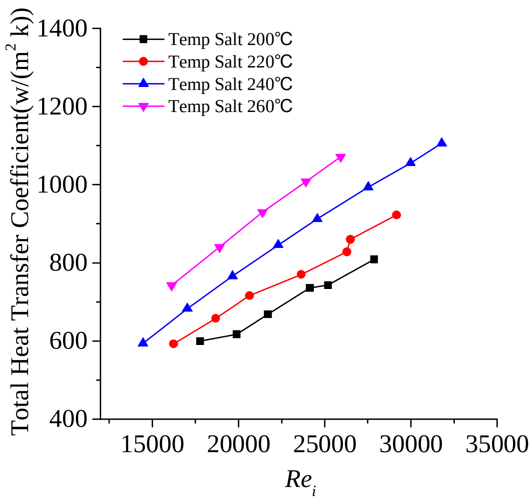

Fig. 5. Total heat transfer coefficient of the exchanger as the salt *Re* changes

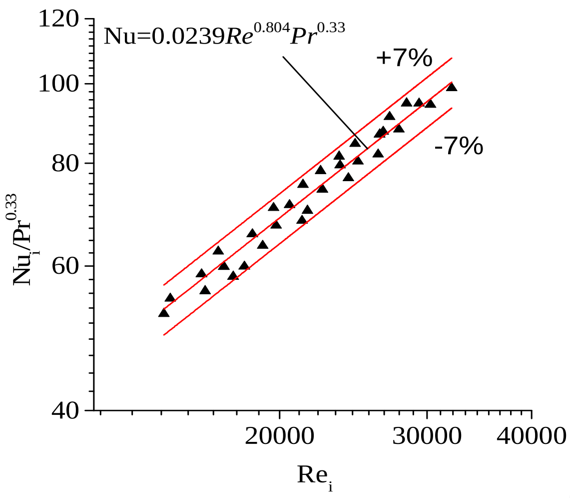

Fig. 6. Fitting curve of the molten salt *Nu* and relative errors

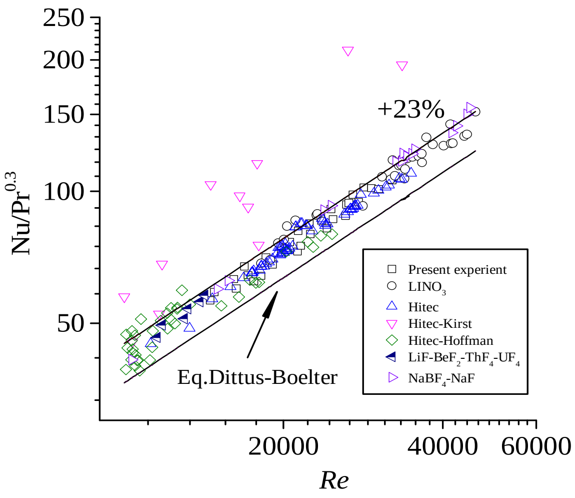

Fig. 7. Comparison of present experimental results, existing data, and the Dittus-Boelter equation

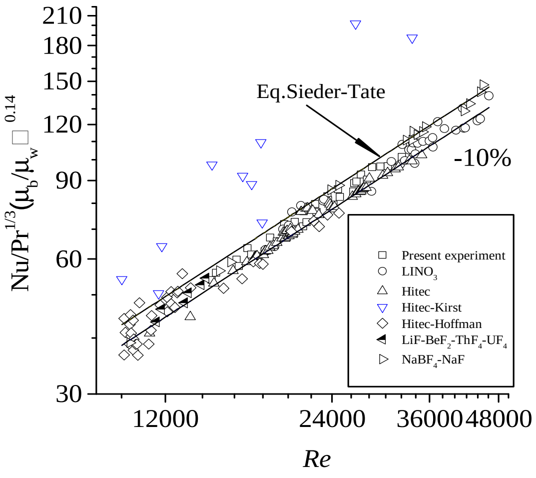

Fig. 8. Comparison of present experimental results, existing data, and the Sieder-Tate equation

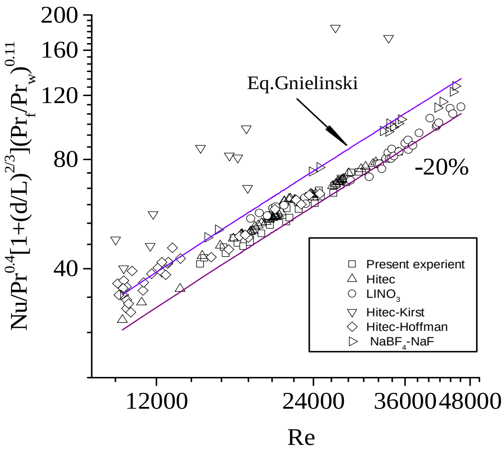

Fig. 9. Comparison of present experimental results, existing data, and the Gnielinski equation

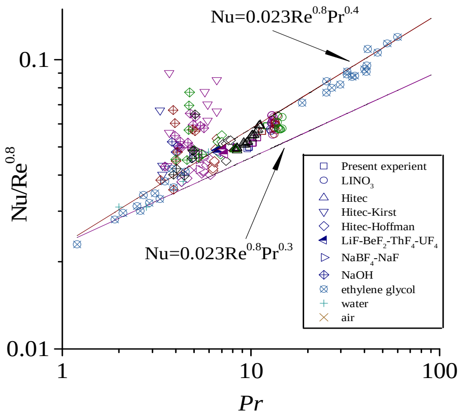

Fig. 10. Prandtl number dependence of the Nusselt number of turbulent flow in a circular tube

Highlights

- A low melting point molten salt was applied in CSP systems.
- Experiment indicates a low risk of freezing and plugging.
- The results show the proportion of the thermal loss at the joints.
- Total heat transfer coefficient of the water-to-salt heat exchanger was obtained.